

Tropical Rainfall Trends from GPCP Analyses

Y. P. Zhou¹, K.-M. Lau²

¹Goddard Earth Sciences & Technology Center, University of Maryland Baltimore County, Catonsville, MD

²Laboratory for Atmospheres, NASA Goddard Space Flight Center, Greenbelt, MD

Abstract

The monthly and pentad GPCP-precipitation data from 1979 to present are analyzed to obtain trends in the tropical hydrological cycle over the last three decades. Results show that tropical precipitation has intensified in the rising regions of the Walker and Hadley circulations while the relatively dry subsidence regions have become drier. In addition, the precipitation PDF has shown distinct signatures for the tropical oceans and land. The tropical oceans present an artificial shift in PDF toward more heavy rainfall around 1987 due to the inclusion of SSM/I data in the merged product. The tropical land does not show significant shift in PDF due to the contribution of many gauge observations. Trend analysis of the top 10% heavy rainfall in the pentad data shows that tropical oceans present an overall positive trend of 1.17 mm/day/decade for the last three decades after removing the artificial jump in the pre-SSM/I data. Precipitation from tropical land shows large decadal variation and presents a smaller positive trend of 0.68 mm/day/decade. The Tropics as a whole displays a positive trend of 1.03 mm/day/decade in the top 10% heavy rainfall.

Keywords: Precipitation, tropical hydrological cycle, global warming

1. Introduction

One important aspect of climate change with increasing greenhouse gases is the change of the hydrological cycle [Meehl et al., 2007; Allan and Soden, 2007]. The response of global precipitation is largely constrained by radiative-convective balance of the troposphere [Allen and Ingram, 2002]. Changes in precipitation distribution and characteristics are as vital to the society as the total amount [Trenberth et al., 2003], and may occur with or without changes in total precipitation [New et al., 2001]. Climate models predict a mild increase of total precipitation but a much more significant increase of extreme events [Palmer and Räisänen, 2002; Kharin and Zwiers, 2005; Meehl et al., 2005; Sun et al. 2007]. Some observational studies also found increases in intense precipitation events in the last century or decades [Dai et al., 1997; Karl and Knight, 1998; Easterling et al., 2000; Groisman et al., 2005]. But most of these studies are based on global or regional land precipitations due to the lack of long-term observations over the oceans.

Meanwhile, because atmospheric moisture increases at a faster rate than the precipitation or evaporation, slightly weaker tropical overturning circulation is expected in a warmer climate [Knutson and Manabe, 1995; Held and Soden, 2006]. However, a weaker tropical overturning circulation does not necessarily imply a weaker tropical hydrological cycle [Zhang and Song, 2006; Wang and Lau, 2006; Allan and Soden, 2007; Lau and Wu, 2007; Sud et al. 2008]. The tendency of rainfall to increase in climatologically wet convergence zones and to decrease in dry subsidence regions—the rich-get-richer

mechanism has been noticed and examined in a number of studies [and Held and Soden, 2006; Chou et al. 2009].

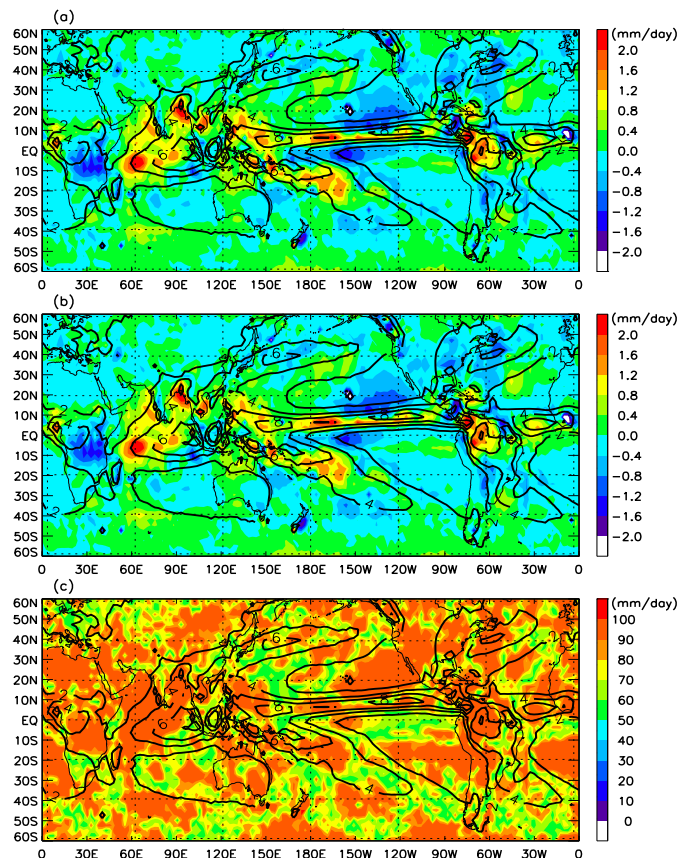
In this study, we will examine different aspects of the trends in the tropical hydrological cycle employing the Global Precipitation Climatology Project (GPCP) monthly and pentad precipitation data sets. GPCP is a community-based analysis of global precipitation under the auspices of the World Climate Research Program (WCRP) from 1979 to the present [Adler *et al.*, 2003; Xie et al. 2003; Huffman et al. 2001]. Archived at 2.5°×2.5° grid, the data combines rainfall estimates from various satellites including microwave-based estimates from Special Sensor Microwave/Imager (SSM/I), infrared (IR) rainfall estimates from geostationary and polar-orbiting satellites, and surface rain gauges. To mitigate the possible data inhomogeneity due to changes in satellites and rainfall algorithms, especially the addition of SSM/I instruments after 1988, GPCP has been designed to preserve temporal homogeneity maximally. The monthly GPCP has been cross-calibrated before 1988 (pre-SSM/I) with later period (post-SSM/I) based on an overlapping period to minimize the systematic bias [Adler et al., 2003]. The pentad GPCP is matched to the monthly GPCP in that the pentad approximately sums to the monthly estimate. However, this calibration is not likely to eliminate all the biases with respect to inhomogeneity at time scales shorter than one month. We will address the artificial jump in the data when estimating trends from these data sets.

2. Change of precipitation distribution associated with tropical overturning circulations

To compute the geographical distributions of precipitation trends, first we computed monthly precipitation anomalies using GPCP monthly data. Two kinds of precipitation anomalies were computed, one by subtracting the monthly climatology and thus the mean annual cycle from the data (called Anom-I), another by further removing ENSO effect using regression to the Nino3.4 index (called Anom-II). The monthly anomalous time series are summed to seasonal and annual time series and a linear trend was computed for each grid box. Figure 1 shows the geographical distribution of trend in annual precipitation (background shaded) computed with Anom-I (Figure 1a) and Anom-II (Figure 1b) for the tropics and the map of confidence level (background shade) from student t-test for Anom-II over the last 29 years (1979-2007). The climatology of the same period is superimposed as contours in the figures. It is found that the majority of the tropical areas exhibit trends of increasing precipitation; the strongest positive trends are seen in the heavy precipitation areas, i.e., ITCZ, SPCZ, Indian-Pacific warm pool, and the Amazon regions, while the strongest negative trends are noted over the light precipitation area, i.e., at both edges of the ITCZ, south of equatorial Africa (Figure 1a). The ENSO-removed trend map shows very similar spatial pattern with the one that contains ENSO effect, with slightly stronger trends in the areas with large positive and negative trend (Figure 1b). The majority of the areas show above 90% confidence level, especially in the subtropical sinking area in northeast Pacific, tropical Indian Ocean and African continent (Figure 1c). Thus wet (dry) regions are tending to be wetter (drier), in agreement with previous studies [Allan and Soden, 2007; Chou et al., 2007; Lau and Wu, 2007; Zhang et al., 2007]. In the following, we will examine precipitation trends associated with Walker circulation and Hadley circulation.

A. Precipitation distribution associated with the Walker circulation

Precipitation changes associated with the Walker circulation were examined for all seasons using the meridional averaged (30°N-30°S) precipitation for each season and the year. Figure 2 shows a time-longitude plot of MAM precipitation averaged from 30°N to 30°S and the corresponding trend for each longitude. The heavy (light) precipitation over the Western (Eastern) Pacific Ocean corresponds with the rising (sinking) branches of the Walker circulation and the areas of positive (negative) trend. Despite large interannual variability, Table 1a shows that linear trends of precipitation (computed from Anom-I data) over the rising (120°E-180°E) and sinking (150°W-100°W) regions of the Pacific Walker circulation are positive and negative, respectively for all the seasons and the yearly average, with the MAM and JJA seasons having



the largest positive trends (95% c.l. based on student t-test) (Table 1a). The precipitation trends computed from Anom-II time series (with ENSO effects removed) shows the same positive (negative) trends in the rising (sinking) regions of the Walker circulation, with slightly smaller magnitude in the trend for the DJF, MAM, and SON seasons but generally improved statistical significance, especially for the MAM and SON seasons in the sinking region (Table 1b).

magnitude in the trend for the DJF, MAM, and SON seasons but generally improved statistical significance, especially for the MAM and SON seasons in the sinking region (Table 1b).

B. Precipitation distribution associated with Hadley circulation

The changes in precipitation distribution associated with the Hadley circulation were investigated using zonally averaged precipitation. The time-latitude plot of the annual mean precipitation shows a large band of high precipitation in the ascending region of the ITCZ and a band of small precipitation in the subtropical subsidence region(s) (Figure 3a). The corresponding latitudinal trend shows positive trend between 15°S-25°N and peaks around 5°N where ITCZ rains most but negative trend at subtropical sinking region(s) (Figure 3b). The negative trend in the northern hemisphere extends further north to about 55°N which is likely due to decreases of precipitation associated with

middle latitude storm track and northward shift of Hadley circulation (Lu et al., 2007). There are large seasonal and regional variations in terms of the boundaries of ITCZ and Hadley circulation, here only annual mean precipitation is considered.

Table 1. Precipitation trends associated with the Walker circulation in the rising (30°S-30°N, 120°E-180°E) and sinking (30°S-30°N, 160°W-100°W) regions a) with ENSO signal, b) ENSO signal removed. Bold font indicates c.l. greater than 90%, star indicates c.l. greater than 95%.

Trend (mm/day/decade)	DJF	MAM	JJA	SON	Year
(a) With ENSO signal					
Rising region	0.067	0.185*	0.118*	0.092	0.116*
Sinking region	-0.050	-0.104	-0.040	-0.097	-0.072
(b) ENSO signal removed					
Rising region	0.048	0.171*	0.127	0.081	0.106*
Sinking region	-0.027	-0.086*	-0.050	-0.083*	-0.061*

Using a similar method as for the Walker circulation, the annual precipitation trends for the tropical rising region (17.5°S-17.5°N) is 0.94 mm/day/decade with 99% c.l., and -0.15 mm/day/decade for both the southern (35°S-17.5°S) and northern (17.5°N-40°N) branches of the sinking region with 90% c.l. This increasing rainfall in the rainy ITCZ region and decreasing rainfall in the dry subtropical sinking region(s) indicates strengthening of the hydrological cycle in the tropics.

3. Changes in rainfall PDF

Changes of precipitation characteristics are not only evident in its spatial distribution, but also in frequency and

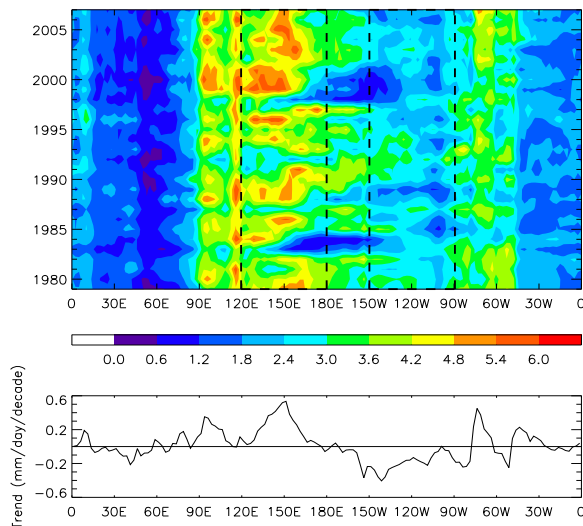


Figure 2. Time-longitude distribution of meridionally (0-30°N) averaged GPCP precipitation for MAM season from 1979-2007 (image). Regions of rising (sinking) area of the Walker circulation are marked in box. The line plot shows the linear trend of meridionally averaged precipitation with longitude.

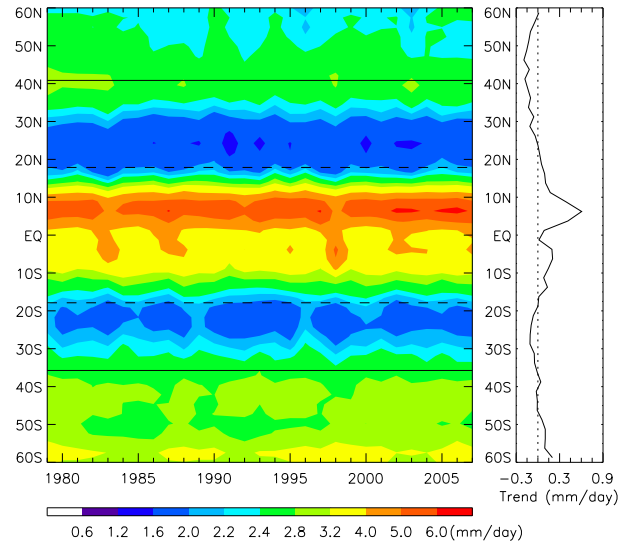


Figure 3. Zonal averaged annual GPCP precipitation from 1979 to 2007 (images). The line plot on the right shows linear trend of zonal averaged precipitation.

because of its higher temporal resolution. Lau and Wu [2007] analyzed the pentad GPCP and CMAP (the CPC Merged Analysis of Precipitation) data sets and found a significant shift in the rainfall distribution that indicates positive trends in extreme heavy and light rains, and a negative trend in moderate rain in the tropics. Here we will focus on extreme rain in the tropical ocean and land and the impact of data inhomogeneity to the derived trend. We first computed the climatological precipitation PDF for the rain frequency and amount from gridded pentad data for the tropical area (30°S-30°N), tropical oceans, and tropical land, respectively, for the entire period 1979-2007. Similar yearly PDFs are computed from data of individual years. Normalized anomalies in PDF for each year are then computed from yearly PDF and the climatological PDF.

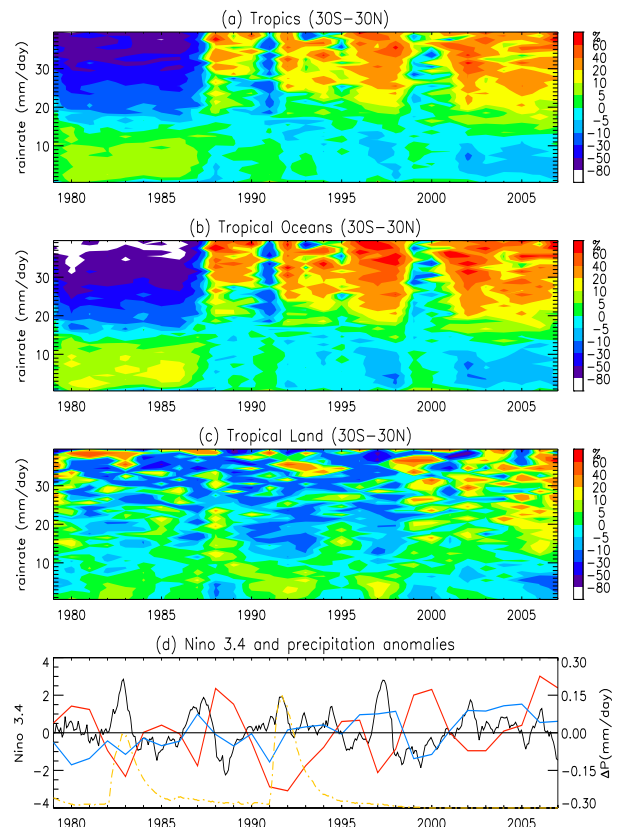
Figure 4 shows the percentage anomaly of annual rainfall PDF for the entire tropics, tropical oceans and tropical land. The characteristics of PDF over the ocean are similar to that of the entire tropics. This is because ocean occupies 72% of the total tropical area and approximately 73% of the total rainfall amount, so that the precipitation time series for the total tropics resembles that of tropical oceans. One striking feature of the figure is the abrupt change of the PDF around mid-1987 in the Tropics and Tropical oceans that coincides the inclusion of SSM/I microwave measurements in the GPCP processing (Figure 4a, 4b). Prior to 1988, the rainfall spectrum shows above-average PDF for rain rate below 15 mm/day and well

intensity distribution that can be described with probability distribution function (PDF). To examine the change of precipitation PDF in the Tropics in recent decades, the pentad GPCP data is analyzed instead of monthly GPCP

below-average PDF for rain rate greater than 15 mm/day. The feature reverses in 1988. This abrupt shift in PDF is not noticeable in the tropical land (Figure 4c). Satellite retrieval over land is less reliable than over ocean but is compensated by merging abundant rain gauges over land. Over the global land area, there are over 6000 Global Telecommunication System (GTS) stations in contrast to over 100 over the ocean, which are located on atolls and small islands mainly in the central and western tropical Pacific Ocean. The gauge observations have been blended into GPCP to not only improve the total rainfall amount but also the rain frequency and distribution [Xie et al., 2003]; meaning that the merged data is less affected by the inclusion of SSM/I data.

The interannual variability of the rain spectrum for the period beginning 1988 can largely be attributed to ENSO and volcanic effects. El Niño is generally associated with more heavy rain (1988, 1997 and 2002) and La Niña the opposite (1995, 1999-2001) (Figure 4a). The ENSO also has quite an opposite effect on rainfall spectrum between the land and ocean. The positive phase of ENSO is associated with more heavy rain in the ocean and less over land, a response similar as total precipitation [Curtis et al., 2007; Gu et al., 2007]. Two major volcanoes erupted during the period, the El Chichon in 1982 and Pinatubo in 1991, both coincident with an El Niño event and masking the ENSO signal. The effect of El Chichon and ENSO events can barely be discerned before 1988 in tropics and tropical oceans. The sharp decrease in heavy rain in 1991 is mainly due to Pinatubo which is also evident in total tropical rainfall [Gu et al., 2007]. Besides the large interannual variability, the PDF seems to shift toward heavy rain starting in 1988 in tropics and tropical oceans but around 1999 in tropical land. The increase in heavy precipitation is in unison with increase in total precipitation [Easterling et al., 2000].

The above results suggest that the PDF of the GPCP pentad precipitation has an artificial jump around 1988 that could be largely attributed to the inclusion of SSM/I with the effect most noticeable over the tropical ocean. It seems that the calibration using the overlapping period may have corrected the monthly total bias [Adler et al., 2003] but is less effective on the rainfall PDF. Since the PDF of the tropical land shows a change around 1999, we further examined the trend in the PDF of the Climate Prediction Center global pentad gauge analysis which is used in the merged product. The result indicates no obvious problem in the land product (figures not shown), which means that this apparent change in PDF of land is less likely an artificial change. Similar shifts in PDF have been found in the monthly GPCP data (figures not shown). Thereafter, the seemingly increasing heavy rain in rainfall PDF could be a real trend in the tropical climate, part of multi-decadal oscillation or because different products are having different degrees of influence. In the following, we will assess the linear trend in tropical extreme rain with the knowledge of these data problems.

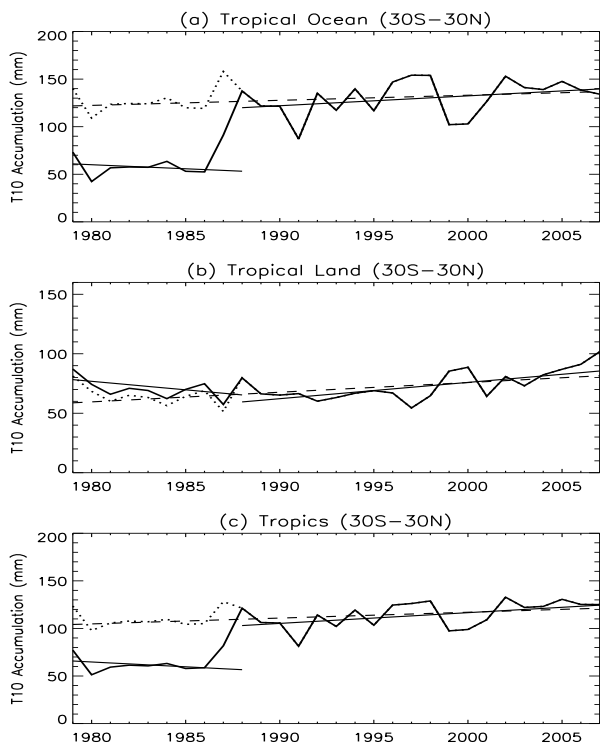


4. Quantitative assessment of trends of extreme rainfall in tropics

One way to quantify the trend in precipitation PDF is to examine the yearly accumulated precipitation in different rain categories [Lau and Wu, 2007]. Here we

Figure 4. Percentage anomalies in yearly precipitation PDF for the (a) entire tropics, (b) tropical oceans, and (c) tropical land. The bin size of precipitation PDF is 1 mm/day. (d) Time series of Nino 3.4 index (black line), global mean stratospheric aerosol optical thickness (dashed orange line, scale from 0 to 0.2) and precipitation anomalies for the tropical oceans (blue line) and tropical land (red line).

examined the linear trend of the top 10% (T10) precipitation to study the trend in extreme rain in the Tropics. Note that extreme rain based on pentad and $2.5 \times 2.5^\circ$ grid data are not instantaneous rain or rain from a single storm in conventional definition, but an extreme wet period in a large area, possibly due to more frequent rain events or larger and lingering rain system in the area in the 5-day period. The T10 rain threshold based on all years over the entire tropics is 22 mm/day, representing roughly about the top 1% of all rain events. Similar results are found for the top 20% and top 30% precipitation (not shown). The yearly accumulations of T10 over the entire tropics, and those over tropical ocean and land are shown in Figure 5. As expected, the T10 over ocean and over the entire tropics nearly doubled across the 1988 boundary.



The T10 from the tropical land varies slowly over the years.

To remove the artificial shift in the T10 rain around mid-1987, we computed linear trends for the pre-SSM/I period 1979-1987 and post-SSM/I period 1988-2007 (shown as solid straight lines) respectively, and computed Figure 5. Annual accumulation of rain in top 10% category for entire tropics, tropical oceans and tropical land (solid thick lines). Solid straight lines indicate linear trends for period 1979-1987 and 1988-2007, dotted line indicate adjusted time series for the period 1979-1988. Dash lines indicate linear trend for the entire period for the adjusted time series.

the artificial shift of the two periods as the difference of the linear fitting values for 1988 from the pre-SSM/I and post-SSM/I time series. The estimated shift is then added to the pre-SSM/I period (dotted line) and a linear trend is computed from the reconstructed time series for the entire period. For the tropical oceans, both periods show positive trends with slightly different magnitude, and the trend for the entire period is 1.17 mm/day/decade with 99.6% c.l.. For the tropical land, although the shift in the time series is minimal, the pre-SSM/I period presents a negative trend of 1.97 mm/day/decade while the latter period presents a positive trend of 1.37 mm/day/decade which indicates large decadal variations in the land precipitation. However, the overall trend for the reconstructed time series still presents a 0.68 mm/day/decade positive trend with 97.8% c.l.. For the entire Tropics, the pre-SSM/I period has a small non-significant positive trend due to opposite signs in the land and ocean time series and a significant positive

trend in the post-SSM/I period. The reconstructed time series for the entire period has a positive trend of 1.03 mm/day/decade with 99.9% c.l.

5. Summary and Discussion

Our investigation employing GPCP data shows that tropical precipitation trends are dominated by increasing contrasts between dry and wet regions, the wet regions are getting wetter while the dry regions are getting drier as also seen in GCM simulations by Held and Soden [2006, Chou et al. 2009]. The tropical Pacific shows increasing (decreasing) precipitation trends in the rising (sinking) regimes of the Walker circulation. Precipitation trends associated with the Hadley circulation also show increasing (decreasing) trends in the wetter ITCZ (drier subtropical) regions.

In addition, precipitation PDF has shown distinct signatures for the tropical oceans and land. An artificial shift in precipitation PDF in the Tropics is identified when SSM/I precipitation estimates begin to be included in July 1987. The disparity is less noticeable over the tropical land due to the contributions of many rain gauge observations. The careful calibration between data periods for the monthly product has prevented spurious variations in the total precipitation [Adler et al., 2003; Smith et al., 2006], but was not designed to eliminate the artificial shift in PDF. Trend analysis of the top 10% heavy rainfall in the pentad data shows that tropical oceans present an overall positive trend of 1.17 mm/day/decade for the last three decades after removing the artificial jump in the pre-SSM/I data. The tropical land shows large decadal variations and presents a smaller positive trend of 0.68 mm/day/decade. The Tropics as a whole presents a positive trend of 1.03 mm/day/decade in the top 10% heavy rainfall. All these trends are significant at 95% level. The shift in PDF towards a positive trend in heavy rain for the entire tropics is consistent with the previous results [Lau and Wu 2007]; however, the trend is weaker than that found in the previous study. A similar PDF shift has been found in GPCP monthly product although the exact mix of satellite and the merge algorithm for it are different from the pentad product.

We should note that our current analysis is subject to further evaluation of possible systematic bias due to changes in characteristics of different satellite products. The time series is also too short to resolve multi-decade variability. Nevertheless, we stress that changes in tropical hydrological cycle might be well underway. Lengthening the record of high-quality precipitation is essential to resolving the uncertainties in today's climate record.

References

- Adler, R. F. and Coauthors, 2003: "The version 2 Global Precipitation Climatology Project (GPCP) Monthly Precipitation Analysis (1979-present)", *J. Hydrometeor.*, **4**, 1147-1167.

- Allen, M. R. and W.J. Ingram, 2002: "Constraints on future changes in climate and the hydrologic cycle", *Nature*, **419**, 224-232.
- Allan, R. P., and B. J. Soden, 2007: "Large discrepancy between observed and simulated precipitation trends in the ascending and descending branches of the tropical circulation", *Geophys. Res. Lett.*, **34**, L18705, doi:10.1029/2007GL031460.
- Chou, J., J. D. Neelin, C.-A. Chen, J.-Y. Tu, 2009: "Evaluating the 'Rich-Get-Richer' mechanism in tropical precipitation change under global warming", *J. Climate*, **22**, 1982-2005
- Curtis, S., A. Salahuddin, R.F. Adler, G.J. Huffman, G. Gu, and Y. Hong, 2007: "Precipitation extremes estimated by GPCP and TRMM: ENSO relationships", *J. Hydrometeorol.*, **8**, 678-689.
- Dai, A., I. Y. Fung, and A. D. Genio, 1997: "Surface observed global land precipitation variations during 1900-88", *J. Climate*, **10**, 2943-2962.
- Easterling, D. R., J. L. Evans, P. Ya. Groisman, T. R. Karl, K. E. Kunkel, and P. Ambenje, 2000: "Observed variability and trends in extreme climate events: A brief review", *Bull. Am. Meteorol. Soc.*, **81**, 417-425.
- Groisman, P. Y., R. W. Knight, D. R. Easterling, T. R. Karl, G. C. Hegerl, and V. N. Razuvaev, 2005: "Trends in intense precipitation in the climate record", *J. Climate*, **18**, 1326-1350.
- Gu, G. J., R. F. Adler, G. J. Huffman, and S. Curtis, 2007: "Tropical rainfall variability on interannual-to-interdecadal and longer time scales derived from the GPCP monthly product", *J. Climate*, **20**, 4033-4046.
- Held, I. M., and B. J. Soden, 2006: "Robust responses of the hydrological cycle to global warming", *J. Climate*, **19**, 5686-5699.
- Huffman, G.J., R. F. Adler, M. Morrissey, D.T. Bolvin, S. Curtis, R. Joyce, B. McGavock, J. Susskind, 2001: "Global precipitation at one-degree daily resolution from multi-satellite observations", *J. Hydrometeorol.*, **2**, 36-50.
- Karl, T. R. and R. W. Knight, 1998: "Secular trends of precipitation amount, frequency, and intensity in the United States", *Bull. Am. Meteorol. Soc.*, **79**, 231-241.
- Kharin, V.V., and F.W. Zwiers, 2005: "Estimating extremes in transient climate change simulations", **18**, 1156-1173.
- Knutson, T. R., and S. Manabe, 1995: "Time-mean response over the tropical Pacific to increased CO₂ in a coupled ocean-atmosphere model", *J. Climate*, **8**, 2181-2199.
- Lau, K. M., and H. T. Wu, 2007: "Detecting trends in tropical rainfall characteristics, 1979-2003", *Int. J. Climatol.*, **27**, 979-988.
- Lu, J., G. A. Vecchi, and T. Reichler, 2007: "Expansion of the Hadley cell under global warming", *Geophys. Res. Lett.*, **34**, L06805.
- Meehl, G. A., J. M. Arblaster, and C. Tebaldi, 2005: "Understanding future patterns of increased precipitation intensity in climate model simulations", *Geophys. Res. Lett.*, **32**, L18719, doi:10.1029/2005GL023680.
- Meehl, G. A., and Coauthors, 2007: Global climate projections. *Climate Change 2007: The Physical Science Basis*, S. Solomon et al., Eds., Cambridge University Press, 747-845.
- New, M., M. Todd, M. Hulme, P. Jones, 2001: "Precipitation measurements and trends in the twentieth century". *J. Climat.*, **21**, 1899-1922.
- Palmer, T. N. and J. Räisänen, 2002: "Quantifying the risk of extreme seasonal precipitation events in a changing climate", *Nature*, **415**, 512-514.
- Santer B. D., T. M. L. Wigley, J. S. Boyle, D. J. Gaffen, J. J. Hnilo, D. Nychka, D. E. Parker, and K. E. Taylor, 2000: "Statistical significance of trends and trend differences in layer-average atmospheric temperature time series". *J. Geophys. Res.*, **105**, 7337-7356, D6.
- Smith, E. A., and coauthors, 2007: International Global Precipitation Measurement (GPM) program and mission: An overview. *Measuring Precipitation from space: EURAINSAT and the Future*, V. Levizzani, P. Bauer, and F. J. Turk, Eds., Springer, 611-654.
- Smith, T. M., X. Yin, and A. Gruber, 2006: "Variations in annual global precipitation (1979-2004), based on the Global Precipitation Climatology Project 2.5° analysis", *Geophys. Res. Lett.*, **33**, 705, doi:10.1029/2005GL025393.
- Sud, Y. C., G. K. Walker, Y. P. Zhou, and W. K.-M. Lau, 2008: "Influence of local and remote sea-surface temperatures on precipitation as inferred from changes in boundary layer moisture convergence and moist thermodynamics over global oceans", *Q. J. R. Meteorol. Soc.*, **134**, 147-163.
- Sun, Y., S. Solomon, A. Dai, and R. W. Portmann, 2007: "How often will it rain?", *J. Climate*, **20**, 4801-4818.
- Trenberth, K. E., A. Dai, R. M. Rasmussen, and D. B. Parsons, 2003: "The changing character of precipitation", *Bull. Amer. Meteor. Soc.*, **84**, 1205-1217.
- Vecchi, G.A., and B. J. Soden, 2007: "Global warming and the weakening of the tropical circulation", *J. Climate*, **20**, 4316-4340.
- Wang, H. and K. M. Lau, 2005: "Hydrologic cycles in the tropics in twentieth century coupled climate simulations", *Int. J. Climatology*, **26**, 655-678.
- Xie P., J. E. Janowiak, P. A. Arkin, R. F. Adler, A. Gruber, R. Ferraro, G. J. Huffman, and S. Curtis, 2003: "GPCP pentad precipitation analyses: An experimental dataset based on gauge observations and satellite estimates", *J. Climate*, **16**, 2197-2214.
- Zhang, M., and H. Song, 2006: "Evidence of deceleration of atmospheric vertical overturning circulation over the tropical Pacific", *Geophys. Res. Lett.*, **33**, L12701, doi:10.1029/2006GL025942.
- Zhang, X., F. W. Zwiers, G. C. Hegerl, F. H. Lambert, N. P. Gillett, S. Solomon, P. A. Stott, and T. Nozawa, 2007: "Detection of human influence on twentieth-

century precipitation trends”, *Nature*, 448, doi:10.1038/nature06025, 461-465.

2010 Hurricane/Typhoon Season Prediction with the NCEP T382 CFS CGCM

Jae-Kyung E. Schemm

Climate Prediction Center, NCEP/NWS/NOAA

Abstract

Since 2009, the Climate Prediction Center has utilized the T382 CFS CGCM forecasts as part of the procedures employed for the Atlantic and Eastern North Pacific hurricane season outlooks. The T382 CFS has shown to have a robust climatological cycle of tropical cyclones (TC) and fair level of skill in predicting the interannual variability of TC numbers over the three Northern Hemisphere ocean basins. The prediction assessments were made based on a series of experimental forecast runs with the T382 CFS CGCM for the storm season of May through November. The experimental runs were made with initial conditions in mid-April during 1981-2008 in the T382 spectral resolution to evaluate tropical storm statistics in the CFS at the highest possible spatial resolution. Tropical storms in the CFS runs were identified using the tropical storm detection method devised by Carmago and Zebiak (2002). Storms depicted in the CFS have very realistic tracks in all four basins in the Northern Hemisphere and a robust seasonal cycle. Comparisons of interannual variability in storm activities indicate that the CFS has reasonable skill and captures the shift to a more active storm era in the Atlantic basin during the post-1995 period.

The 2010 season prediction based on the real time forecast runs of the T382 CFS will be discussed along with the verification of the 2009 storm season.